Attenuation Property of Seismic Waves and Source Characteristics of Small Earthquakes

AUTHOR(S):

AKAMATSU, Junpei

CITATION:

AKAMATSU, Junpei. Attenuation Property of Seismic Waves and Source Characteristics of Small Earthquakes. Bulletin of the Disaster Prevention Research Institute 1980, 30(3): 53-80

ISSUE DATE:

1980-11

URL:

http://hdl.handle.net/2433/124893

Bull. Disas. Prev. Res. Inst., Kyoto Univ., Vol. 30, Part 3, No. 271, November, 1980

Attenuation Property of Seismic Waves and Source Characteristics of Small Earthquakes

By Junpei AKAMATSU

(Manuscript received Oct. 25, 1980)

Abstract

In order to discuss the source characteristics of the local small earthquakes occurring in and around the Kinki district, the attenuation property of body wave is estimated, and the spectral densities are examined through the analysis of the coda parts of the seismograms observed at the Sumiyama Seismic Station in the southern parts of Kyoto.

As for the attenuation of the body waves in the frequency range of 1～20 Hz in the crust, Q increases with frequency quite similarly to that of the coda parts. Q_s is approximated by $Q_s=q\sqrt{f}$, in which $q=110$ for the S travel time, $t_s=5$～50 sec.

It was found that the source spectral density of the far-field shear wave can be explained fairly well by the ω-square model in the range of the magnitude, $M=2$～5. When M is smaller than about 3, the corner frequency of the spectrum takes nearly constant value regardless of the seismic moment. When $M=3$～5, the frequency becomes smaller with increase of the moment. Consequently, according to Brune's model of the dislocation, the stress drop increases from a few bars to several tens of bars with increase of the moment in the low level of the magnitude, $M<3$. While the stress drop is ranging from 10 to 100 bars in relation to the source location and depth in the range of $M=3$～5. In the Kinki district, the seismically active regions, where small and micro earthquakes occur frequently or in a swarm, are characterized by the low stress drop compared with the other non-active regions.

1. Introduction

It is often experienced in seismometry that the predominant periods or the frequency contents of seismic waves vary with the source region as well as with the magnitude. Some regional variations of physical properties such as strength and shear modulus in the upper lithosphere can be examined from the seismic observations. Furuzawa et al. showed that the predominant frequencies of the spectral densities for body waves from the micro-earthquakes vary with the source locations depending on the seismic activity in the southern parts of Kyoto[1]. Hirano examined the source characteristics of small earthquakes, and suggested the regional variation of the stress concentration in the vicinity of Kyoto[2]. As these studies are based on the deterministic way of analysis or Fourier analysis of the short period body waves affected significantly by the fine local geology and topography, suitable smoothing of the spectra or averaging of many observations are necessary.

Recently the analysis of seismic coda has been utilized to study the source characteristics, considering the coda parts as scattered waves by randomly distributed

heterogeneity in the earth[3,4]. The method is based on the empirical relation of the attenuation of the coda, that is, the attenuation of amplitude depends merely on the lapse time measured from the source origin time. And it does not depend on the magnitude, source location, direction of radiation and on the direct wave path from the source to the station, as long as the lapse time is sufficiently longer than the travel time of the direct S waves. From the above observational results the seismic coda is considered to be determined only by the source spectrum and the scattering property of the seismic wave in the upper lithosphere.

The amplitude of the coda, however, must be calibrated with some other seis-

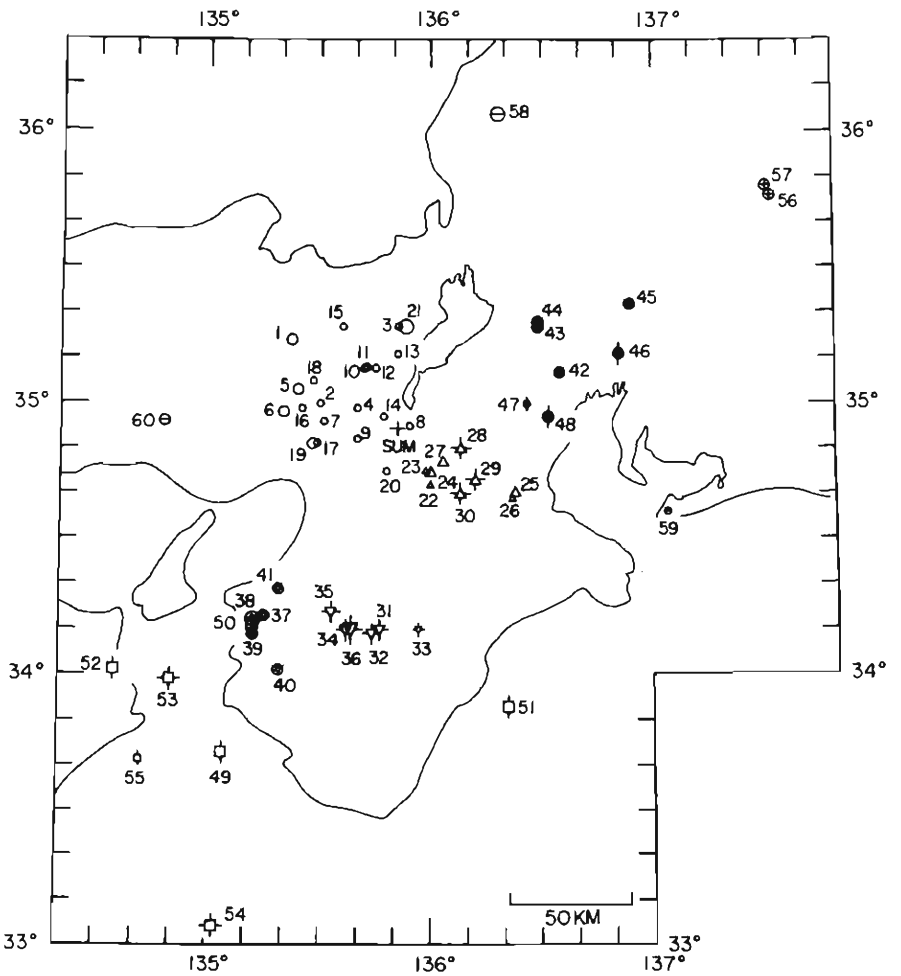

Fig. 1. Epicenters of the events analyzed. SUM denotes the Sumiyama Seismic Station. The range of magnitude are shown by the size of each symbol, small; $M<3.5$, middle; $3.5\leqq M<4.5$, large; $4.5\leqq M$, with the source depth for examples, ○; $H\leqq 30$ km, ⌽; $40\leqq H\leqq 50$ km, ⌖; $H\geqq 60$ km.

mological data to estimate the absolute values of the source parameters such as seismic moment, source dimension and stress drop, because the physical mechanisms of generation and attenuation of the seismic coda are not well understood. Chouet et al. discussed the scaling law of the source spectra and its regional variation[5]. Rautian et al. studied the source characteristics in Garm region with the CHISS spectra[4].

The attenuation property of the seismic coda from the local small earthquakes in the Kinki district was examined in detail in a previous paper[6]. In this paper we examine Q of the body waves from local earthquakes, and discuss the source characteristics of the small earthquakes and their regional variation from the analysis of the coda parts using Q.

2. Attenuation and source factor of coda.

The seismic coda was analyzed with the band pass filtered rms amplitudes $A(f, t)$, which were derived by the ac level meters, as described fully in the previous paper[6]. The events analyzed are listed in Table 1, in which the events are grouped with the source locations. The locations of the sources given by JMA are shown in Fig. 1. Fig. 2 shows the frequency responses of the seismograph system at the Sumiyama Seismic Station and the band pass filters used for the analysis.

The rms amplitude $A(f, t)$ is approximated fairly well by the following functional form of the lapse time, t, measured from the source origin time, when t is larger than 3 times the travel time of the direct S wave t_s,

$$A(f, t)=c\, t^{-a}\, e^{-bt}, \qquad \text{for } t > 3\, t_s. \tag{1}$$

Taking the logarithm of both sides, we obtain

$$\ln A(f, t)=C-a \ln t-b\, t, \qquad \text{for } t > 3\, t_s \tag{2}$$

where c, a and b represent the source factor of coda, the geometrical spreading factor and the attenuation coefficient, respectively. An example of the analysis is shown

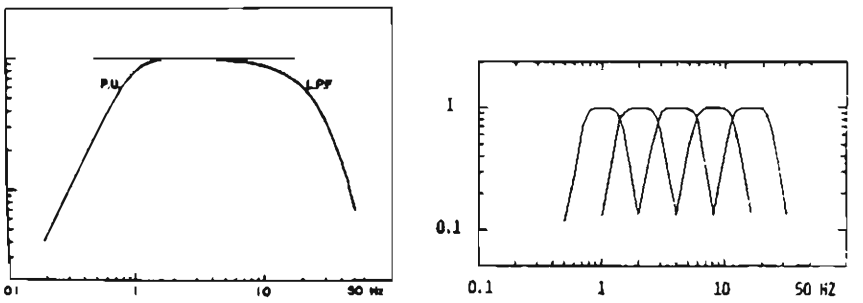

Fig. 2. Frequency responses of the seismograph system and the band pass filters, the center frequencies of which, f_0, are 1, 2, 4, 8 and 16 Hz with the band width of $(\sqrt{2}/2) f_0$. The center frequencies of the lowest and highest bands for the total responses are 1.2 and 14 Hz, respectively.

Table 1. List of the Earthquakes Analyzed and the Source Parameters Estimated.

No.	Year Code	Date	Time		Epicentral distance	Azimuth	Depth	Magnitude	Moment dyne cm	Corner frequency	Radius of source	Stress drop	Region
			H	M	Km	N°E	Km	M	M_0	Hz	Km	bar	
1	76- 264	Sept. 14	21	42	57	−50	10	4.2	4.8×10^{21}	3.2	0.41	38	
2	76- 496	Nov. 13	21	29	34	−72	10	3.3	4.5×10^{20}	5.6	0.23	16	
3	77- 431	July 27	15	04	42	0	20	2.9	4.4×10^{20}	4.6	0.28	8.8	
4	77- 678	Aug. 23	17	38	18	−62	20	3.2	1.0×10^{21}	3.9	0.33	12	
5	77-1316	Nov. 25	12	53	44	−68	10	3.8	1.9×10^{21}	3.6	0.36	18	
6	78- 24	Jan. 7	6	01	47	−81	10	4.0	2.7×10^{21}	4.2	0.31	40	
7	78- 604*	June 13	2	07	30	−84	10	2.8	2.2×10^{20}	5.7	0.23	7.9	
8	78- 656*	June 29	19	32	5	76	10	2.8	2.5×10^{20}	5.1	0.26	6.2	
9	78- 731	July 29	17	32	17	−105	10	2.9	5.9×10^{20}	4.5	0.29	11	
10	78- 789*	Aug. 22	17	51	29	−28	10	2.9	2.5×10^{20}	4.8	0.27	5.6	
11	78- 790	Aug. 22	20	39	29	−28	10	3.4	8.9×10^{20}	4.2	0.31	13	Yodogawa seismic zone
12	78- 794*	Aug. 23	5	55	27	−20	20	2.7	8.5×10^{19}	(10)	(0.13)	(17)	
13	78- 900*	Sept. 25	3	04	31	0	10	3.3	9.1×10^{20}	4.0	0.33	12	
14	78-1341*	Nov. 12	12	35	8	−50	10	2.6	8.3×10^{19}	5.3	0.25	2.3	
15	78-1557*	Dec. 25	10	59	48	−28	10	2.8	1.7×10^{20}	5.9	0.22	7.1	
16	78-1560*	Dec. 26	3	38	40	−78	20	3.1	1.5×10^{20}	(8.0)	(0.16)	(15)	
17	79- 125*	Jan. 26	2	45	34	−100	10	2.6	1.4×10^{20}	5.3	0.25	4.0	
18	79- 503*	Apr. 9	20	49	40	−61	20	2.9	1.7×10^{20}	5.9	0.22	7.0	
19	79- 779	June 1	7	33	35	−100	20	3.6	1.5×10^{21}	3.8	0.34	17	
20	79-1033*	Aug. 18	20	20	18	−160	10	2.3	1.2×10^{20}	5.7	0.23	4.1	
21	79-1186	Oct. 16	7	45	42	5	10	4.9	4.8×10^{22}	2.2	0.61	93	

22	77-1391	Dec.	11	22	39	28	149	0	2.7	1.6×10^{20}	8.6	0.15	21	
23	78- 608*	June	13	22	42	22	145	0	2.7	1.7×10^{20}	8.0	0.16	18	
24	78-1015	Oct.	7	13	18	23	142	0	3.7	2.1×10^{21}	4.2	0.31	31	
25	78-1459	Dec.	5	8	24	56	118	0	4.3	1.2×10^{22}	2.6	0.50	40	
26	79- 252*	Feb.	22	4	18	56	121	0	3.2	4.6×10^{20}	6.8	0.19	29	Iga-Ueno region, Nara and Mie prefectures
27	79- 520	Apr.	12	13	59	24	127	10	4.3	1.3×10^{22}	2.7	0.48	50	
28	78- 219	Feb.	8	3	33	28	107	60	3.8	2.3×10^{21}	4.8	0.27	51	
29	78-1187	Oct.	20	16	00	39	123	60	3.5	1.2×10^{21}	5.6	0.23	41	
30	79-1065	Sept.	12	9	35	38	136	60	3.7	2.0×10^{21}	5.3	0.25	56	
31	76- 584	Dec.	21	8	04	82	−175	60	4.0	3.0×10^{21}	5.0	0.26	75	
32	78- 98	Jan.	16	22	40	85	−173	70	3.5	1.3×10^{21}	4.8	0.27	28	
33	79- 265*	Feb.	24	12	35	83	−173	60	3.3	6.3×10^{20}	6.1	0.21	30	Yoshino region,
34	79- 390	Mar.	16	10	36	85	−166	60	4.0	2.3×10^{21}	5.1	0.26	57	Nara-Wakayama border
35	79- 988	July	31	9	03	81	−160	70	4.0	3.5×10^{21}	3.8	0.34	39	
36	79-1241	Nov.	13	0	42	85	−166	70	4.8	2.5×10^{22}	2.6	0.50	88	
37	76- 609	Dec.	27	10	49	94	−145	0	4.0	5.0×10^{21}	2.4	0.54	14	
38	77- 528	Aug.	7	4	27	98	−143	0	4.5	3.2×10^{22}	1.4	0.93	17	
39	77- 615	Aug.	17	0	32	103	−144	0	4.0	5.5×10^{21}	2.2	0.59	12	Near Wakayama city
40	79- 555*	Apr.	17	20	26	112	−154	0	4.2	6.3×10^{21}	2.2	0.61	12	
41	79-1261	Nov.	21	8	36	83	−144	10	3.8	2.5×10^{21}	2.9	0.46	11	
42	77- 605	Aug.	15	21	03	71	71	20	3.7	1.1×10^{21}	6.3	0.21	52	
43	78-1064*	Oct.	10	3	10	72	53	10	3.8	2.7×10^{21}	4.3	0.30	44	
44	78-1079*	Oct.	10	4	02	71	54	10	3.6	1.9×10^{21}	3.4	0.38	15	
45	79- 299*	Mar.	1	8	13	108	62	0	3.7	1.7×10^{21}	5.1	0.26	41	Aichi, Gifu and Mie prefectures
46	77- 515	Aug.	6	2	44	96	71	50	4.3	1.5×10^{22}	2.8	0.46	67	
47	79- 15*	Jan.	4	16	21	54	79	40	3.2	5.6×10^{20}	6.3	0.21	26	
48	79- 417*	Mar.	21	4	53	63	85	40	3.2	4.4×10^{20}	6.8	0.19	28	

No.	Year Code	Date	Time H	Time M	Epicentral distance Km	Azimuth N°E	Depth Km	Magnitude M	Moment dyne cm M_o	Corner frequency Hz	Radius of source Km	Stress drop bar	Region
49	76- 92	July 18	15	30	150	−151	40	4.3	6.0×10^{21}	3.2	0.41	38	
50	76- 484	Nov. 11	6	05	97	141	40	4.4	1.3×10^{22}	(3.0)	(0.43)	(71)	
51	77-1463	Dec. 22	5	11	123	158	50	4.0	2.3×10^{21}	(4.0)	(0.33)	(28)	Kii Channel and
52	78- 274	Feb. 21	8	19	152	−130	50	4.0	3.4×10^{21}	3.3	0.39	25	in and off Kii Pen.
53	78- 522	May 15	13	35	139	−138	60	4.4	8.7×10^{21}	3.4	0.38	69	
54	78- 635	June 20	1	34	219	−160	60	4.3	5.0×10^{21}	(4.3)	(0.30)	(81)	
55	78-1326	Nov. 7	15	58	172	−141	50	4.4	4.1×10^{21}	3.2	0.41	26	
56	78-1037	Oct. 9	0	00	180	58	0	4.1	6.2×10^{21}	3.9	0.33	75	SW Nagano prefecture,
57	79- 871	June 28	21	29	181	56	10	4.0	3.8×10^{21}	4.5	0.29	68	near the Ontake-volcano.
58	78- 416	Apr. 3	11	04	136	18	10	4.7	3.2×10^{22}	1.8	0.74	35	
59	79- 147	Jan. 30	21	49	117	107	10	3.9	3.0×10^{21}	(4.0)	(0.33)	(37)	Others
60	79-1182	Oct. 13	16	30	95	−97	10	4.3	5.8×10^{21}	3.2	0.41	37	

* denotes the events used for the analysis in the section 3–1 in the text.

in Fig. 3, in which eq. (2) is fitted to each logarithmic rms amplitude using the method of least square. From this procedure we have obtained the following results about the attenuation property of the seismic coda in the frequency range from 1 to 20 Hz for the small earthquakes occuring in the Kinki district; (1) the geometrical spreading factor, a, is $1\sim2$ for $t=15\sim300$ sec, (2) the attenuation coefficient, b, obtained under a condition of $a=1$, depends systematically on the frequency of the pass band, f_0, as well as on the interval of the lapse time used for the analysis, (3) the value of Q derived with $Q=\pi f/b$ is approximated by $Q=160\sqrt{f}$ for $20\leq t\leq60$ sec and $Q=230\sqrt{f}$ for $50\leq t\leq200$ sec[7], (4) the decrease of the attenuation coefficient with the lapse time is interpreted to reflect the layered Q-structure in the upper lithosphere.

The source factor, c, is considered to depend on the source spectral density and the mechanism of wave scattering. Using eq. (2) we may calculate C for each trace of each event. However, as the value of b varies with time, the value of C is changed by the selection of the time interval for the analysis. The dynamic recording range of the seismograph is limited, therefore the available interval of the lapse time varies from event to event, depending on the coda amplitude (or the magnitude). Accordingly the value of C, estimated with eq. (2), has a incorrect value systematically. This argument is obvious in Fig. 3, in which the seismograms of the same event recorded in the high and low gain channels were analyzed with the different time intervals. In order to estimate a correct value of C, we must take account of the

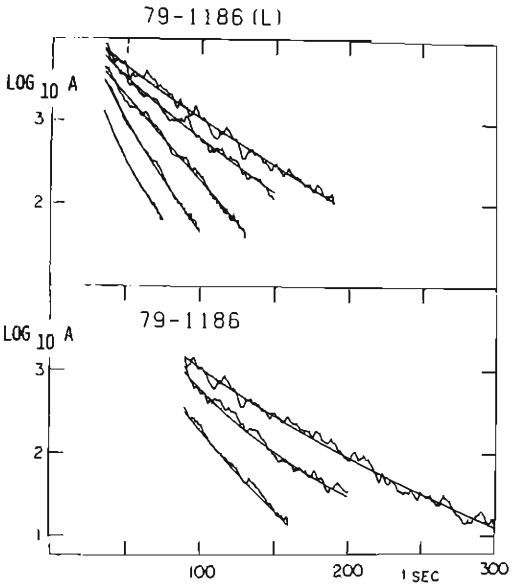

Fig. 3. Examples of the logarithmic rms amplitude log $A(f, t)$ and the decay curves fitted with eq. (2). The event, No. 21, is recorded with two different sensitivities and analyzed with the different time intervals, upper; low gain channel, lower; high gain one.

variation of attenuation with the time. Assuming that the coda part is approximated by the source factor and the general curve of the attenuation for a layered Q-structure, the source factor, C, may be estimated by the following equation,

$$\ln A(f,t)=\begin{cases} C-\ln t-b_1 t, & \text{for } t\leq t_c \\ C-\ln t-b_1 t_c & \\ \quad -b_2(t-t_c), & \text{for } t>t_c \end{cases} \tag{3}$$

, where $b_i=\pi f/Q_i$ $(i=1, 2)$ and t_c is the critical time, and we use $Q_1=160\sqrt{f}$, $Q_2=230\sqrt{f}$ and $t_c=45$ sec. With this procedure the same values of C for the same event are obtainable without depending on the selection of the time interval.

The relation of the growth rates of the source factors in the different frequency bands is shown in Fig. 4, in which the two main tendencies are obvious. First, the growth rate of the component of 1 Hz is larger than those of 8 Hz. This property is due to the fact that the corner frequency, f_c, of the source spectral density lies between those two frequency bands and that f_c decreases with the magnitude, as discussed in the following section.

Secondly, the growth rate of the source factors varies with the source region systematically[7]. The shallow events near Wakayama city (denoted by the symbol ◎ in Figs. 1 and 4) and those in the region near Kyoto from Lake Biwa to Osaka Bay (○) are characterized by the larger amplitude of 1 Hz component than those in the other regions such as Nara and Mie prefectures (△), Gifu and Aichi prefectures (●). The shallow events near Wakayama city are well known to occur in a swarm. The region in the vicinity of Kyoto, where micro-earthquakes occur very frequently, is known by the name of the Yodogawa seismic zone. That is, the predominant frequencies in the source factors vary with the source location in relation with the seismic activity of the regions. On the contrary, the component of

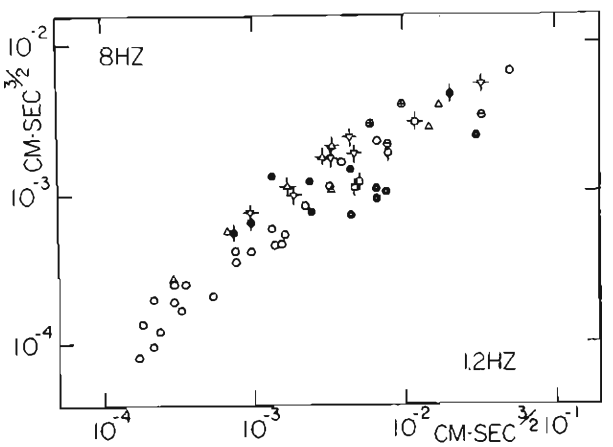

Fig. 4. Relation between the source factors of codas in the different frequency bands and its variation with the source location.

8 Hz is very high in the shallow events near the Ontake-volcano in the SW parts of Nagano prefecture, where small events occur extremely frequently in the narrow region (⊕), showing the different tendency from the above mentioned regions. The deeper events in the region of Yoshino (▽) and Iga-ueno (△) are characterized by the high frequency contents.

The relation between the source factor, C, and the magnitude, M, is shown in Fig. 5. The source factor in each frequency band increases linearly with M in the range of the magnitude from 2 to 5. The rate of increase is larger in the lower frequency band than in the higher one as already seen in Fig. 4. The relation between C and M is considered as equivalent to the relation between the source spectra and M from the property of the coda discussed previously. In Fig. 5 the two ordinates are given with the different units, one of which is for the amplitude level of the coda source factor (in cm·sec$^{3/2}$ unit), and the other is for the source spectral density of the far-field shear wave at the distance of 1 km (in cm·sec unit), which are estimated with the spectral density of SH waves of the reference earthquake with M=2.1, as described in the section 4. The source spectral density of the far-field shear wave normalized to the hypocentral distance of 1 km may be estimated from the source factors of coda for each event and above determined scale in cm·sec unit. In order to construct the reference earthquake, the amount of the attenuation must be known, and is examined through two different ways in the next section.

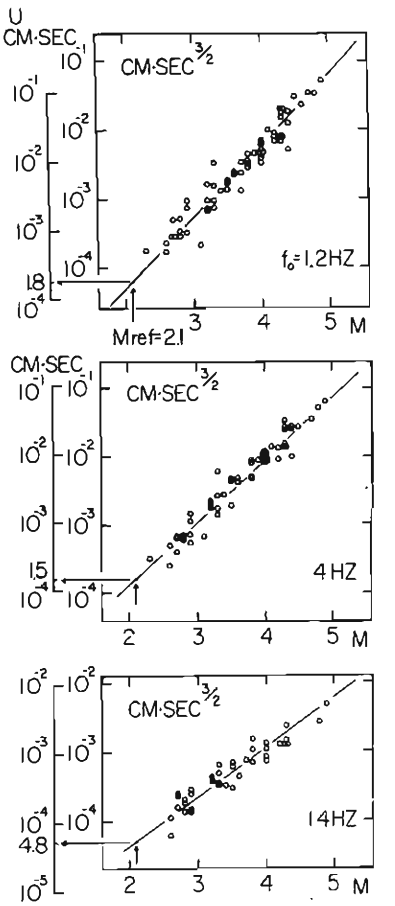

Fig. 5. Growth rate of the coda source factor with magnitude in each frequency band. Note that the source factor increases linearly with magnitude in the range of M=2.3~4.9. The scales for the source spectral density of the far-field shear wave at 1km are added on the left side, which are obtained from the reference earthquake of M=2.1 in Fig. 12.

3. Estimation of Q for body waves and their dependency on frequency.

3–1. Utilization of source factor of coda.

The amplitude of the body wave $A(f)$ is expressed simply as

$$A(f) = S(f, \theta, \varphi)\, R^{-a}\, e^{-\gamma(f)R} \tag{4}$$

, where $S(f, \theta, \varphi)$ is the source spectra for the far-field P or S wave in the direction of (θ, φ). R and a is the path length and the geometrical spreading factor, respectively, and $a=1$ for the body wave. $\gamma(f)$ is the attenuation coefficient, related to Q by $\gamma(f)=\pi f/Qv$, where v denotes the velocity. If the source spectral density is given under some assumption or restricted within a narrow limit, $\gamma(f)$ may be obtainable. For the source spectra Aki et al. used the source factor of coda[3] and Rautian et al. used the coda spectra determined by the envelope at $t=100$ sec[4].

In this analysis we used the source factor of coda obtained in the previous section. As the coda levels are considered to be dependent on the spectral density of the S wave rather than that of P wave, the maximum amplitudes of the band pass filtered S wave were used for $A(f)$ in eq. (4). The sum of the maximum amplitude in the radial and transversal components $\sqrt{A_R^2+A_T^2}$ is used in each frequency band.

The attenuation of $A(f)/c(f)$ is shown in Fig. 6, where the probable attenuation curves are given for each frequency band. Large scattering of $A(f)/c(f)$ is observed in all frequency bands. One of the reasons for the scattering is considered to be

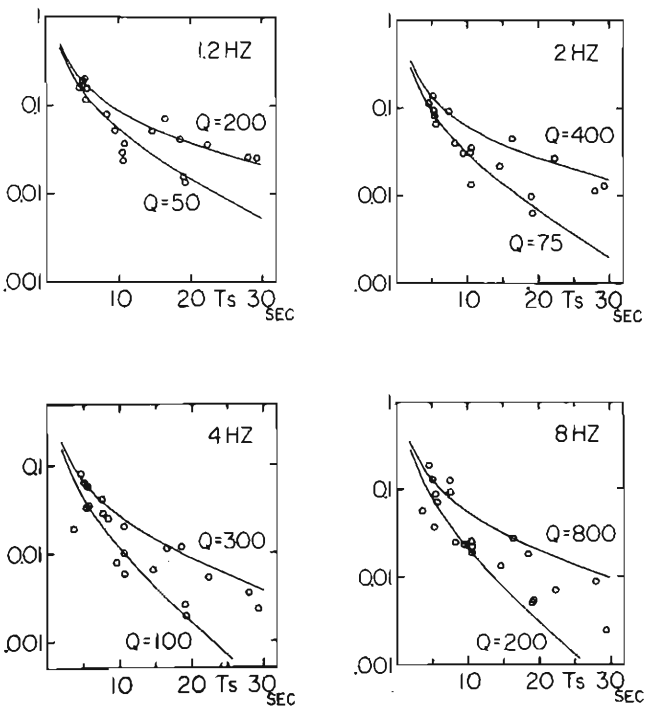

Fig. 6. Attenuation of the S waves with distance. The amplitude is normalized by the corresponding source factor of coda. It is supposed that Q increases with frequency.

Table 2. Q_s^{-1} Estimated with the Source Factor of the Coda.

f_0 Hz	1.2	2.0	4.0	8.0	14
Q_s^{-1} ($\times 10^{-2}$)	0.5—2.0	0.25—1.3	0.33—1.0	0.13—0.5	0.13—0.25

the normalization of the source spectra $S(f, \theta, \varphi)$ with the source factor of coda $c(f)$, only redusing the effect of the magnitude, but not that of the radiation pattern, because the seismic coda has already averaged the term of the radiation pattern. Although the range of Q is rather wide, the dependency of Q on the frequency is thought to exist. At least it is difficult to give any one value for Q appropriate to all frequency bands. The range of Q^{-1} are listed in Table 2. The variation of Q with frequency for S waves is quite similar to that for the coda parts described previously.

3–2. Utilization of the amplitude ratio of the different frequency bands.

Let $A(f)$ be the amplitude of body wave filtered with the band pass filter with the center frequency, f. The amplitude ratio of the different bands, f_1 and f_2, is

$$\frac{A(f_1)}{A(f_2)}=\frac{S(f_1, \theta, \varphi)}{S(f_2, \theta, \varphi)} e^{-\{\gamma(f_1)-\gamma(f_2)\}R} \tag{5}$$

, under the condition that both frequency components come through the same path from the source to the station. Taking the logarithm of both sides;

$$\ln\frac{A(f_1)}{A(f_2)}=\ln\frac{S(f_1, \theta, \varphi)}{S(f_2, \theta, \varphi)}-\{\gamma(f_1)-\gamma(f_2)\}R, \tag{6}$$

The attenuation coefficient $\gamma(f)$ is estimated from the slope of the ratio to the distance, R, using many events, under the assumption of nearly constant values for the ratios of the source spectra for different events.

In the analysis we used shallow events ($H \leqq 70$ km) occurring in and around the Kinki district from July 1976 to Oct. 1979, whose locations and magnitudes are given by JMA. The range of magnitude is from 2.3 to 4.9. The epicentral distances were limited to less than 200 km. The total number of events analyzed was about 250. The distribution of the epicenters is shown in Fig. 7.

For the P wave the maximum amplitude of the first wavelet was read in the vertical component. When the epicentral distance is shorter than about 100 km, the first phase is the direct P wave, while at the larger distance the first phase occasionally becomes P_n. In this case the later phase, P_g, was analized. P and P_g are denoted by the index $P=1$ and 2, respectively, as shown in Fig. 9, where the analyzed phases are pointed out. In any case we used only the events whose wave forms are pulsive and whose maximum amplitudes in all frequency bands appear nearly at the same time. The shallow events near Wakayama city were excluded, because their wave forms are complicated, and the identification of phase is difficult.

The identification of the initial S phase is relatively difficult due to the con-

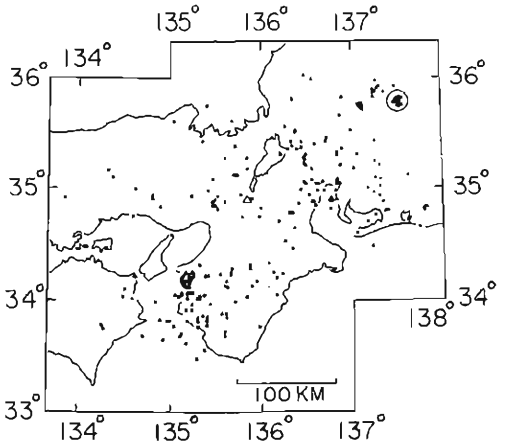

Fig. 7. Distribution of epicenters for the events which are used to analize the amplitude ratios of P and S waves in section 3–2. The events encircled occur very frequently in a swarm near the Ontake-volcano and are characterized by different source spectra.

tamination by P coda and polarization characteristics peculiar to shear wave. In order to identify the initial phase correctly we propose using SH for $A(f)$ as described below.

The direction of the wave propagation, determined with the particle motion analysis of the initial P phase, is nearly identical to the source azimuth within a few degree at the Sumiyama Seismic Station[8]. In the case of S waves, however, the direction of the propagation cannot be estimated by the same analysis because of the S-polarization. However, it is thought that the direction is not deflected seriously from the source azimuth. Therefore the transversal component to the source azimuth is composed using the circuit shown in Fig. 8.

We could not classify S phase such as S_n and S_g as done in the case of P. The analysis was restricted to the pulsive first wavelet in the transversal component. The events were classified into two groups according to the difference of the arrival

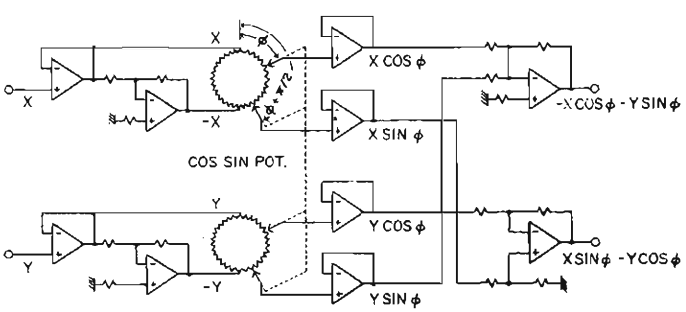

Fig. 8. Circuit diagram of the axis-transformer which generates the radial and transversal components from the two horizontal ones, N–S and E–W.

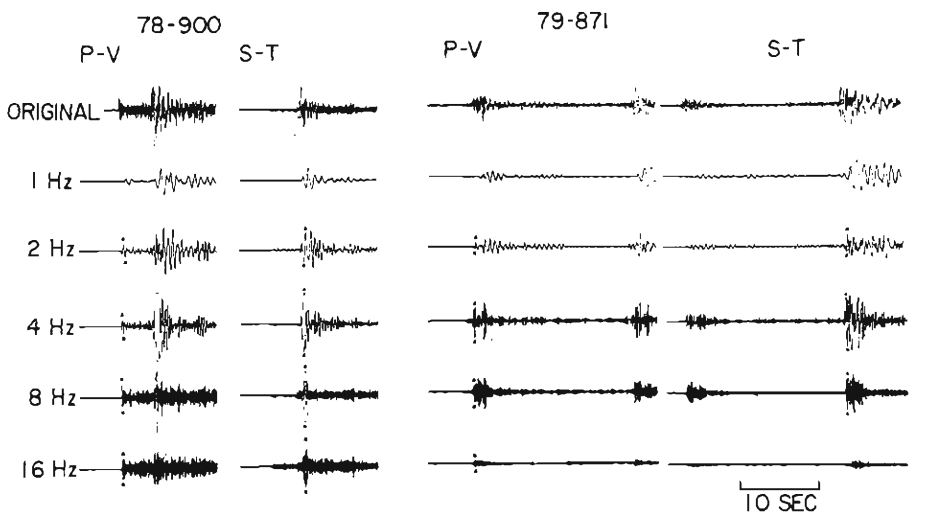

Fig. 9. Examples of the band pass filtered seismograms. Dots show the phases analyzed. Event 78–900: Sept. 25, 3 h 3 m, 1978, φ=N 1° E, $\triangle$=30 km, H=10 km, M=3.3, Index P=1, Index S=1. Event 79–871: June 28, 21 h 29 m, 1979, φ=N 57° E, $\triangle$=181 km, H=10 km, M=4.0, Index P=2, Index S=1. For the meening of the index, see text.

time, t, for the maximum amplitude in all frequency bands, that is, group 1 for $\Delta t \leqq 0.3$ sec (index S=1) and group 2 for $\Delta t \leqq 1$ sec (index S=2). The events with $\Delta t > 1$ sec were excluded to avoid the effect of multi paths. Some examples of these filtered traces are shown in Fig. 9 where the maximum amplitude used for the analysis are denoted.

There are many events having later arivals after about 1 sec for the first wavelets in P and S waves as seen in Fig. 9. In this case the first wavelet in 1 Hz band is distorted by the later one and not used for $A(f)$.

The attenuation of the amplitude ratios in the two sets of the frequencies is estimated as shown in Fig. 10. The distance, R, is given by the epicentral distance, $\triangle$, and the source depth, H, $R=\sqrt{\triangle^2+H^2}$. In the figures the attenuation of ratio with distance is obvious, although there is large scattering in both the case of P and S waves. In the analysis we took care in the phase identification. However, the attenuation property does not vary largely for the different phases.

In the figures of 14 Hz/2 Hz, for P and S, it is remarkable that there are many events with high values at a distance of about 180 km. These events occurred frequently in a swarm near the Ontake-volcano, which are encircled in Fig. 7. As mentioned in the analysis of the coda parts, this region is noticeable because the high frequency content is predominant in the source factor of coda ($\oplus$ in Figs. 1 and 4). In the lower figures (14 Hz/2 Hz) two different slopes are shown, one of which was obtained with all data within 200 km while the other excludes the above region.

The range of magnitude is from 2.3 to 4.9. The growth rates of the coda source

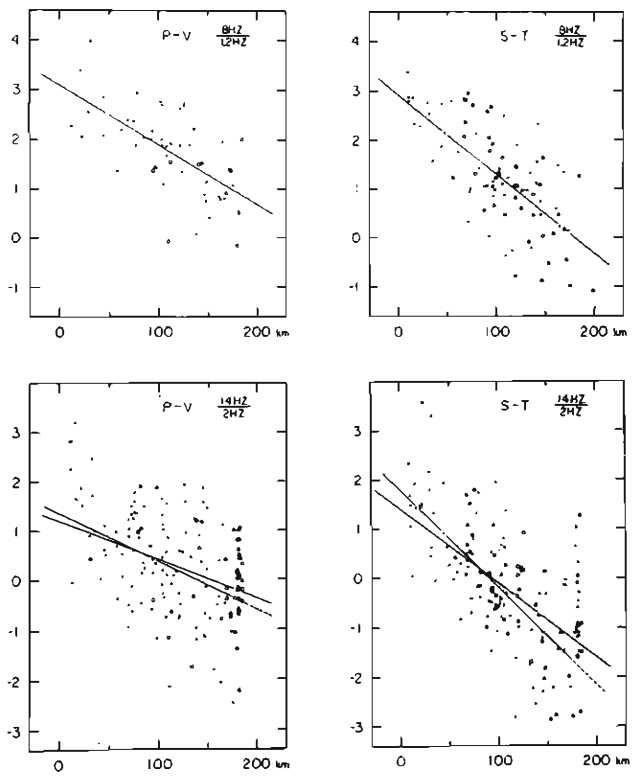

Fig. 10. Attenuation of the amplitude ratios with distance. Dot and open circle denote the phases with index of 1 and 2, respectively. No differences are found in the attenuation property for the phases with different index. The attenuation coefficients are estimated including and excluding the events at $\triangle \simeq 180$ km, which are encircled in Fig. 7.

factors in this range depend on the frequency, suggesting variation of the source spectra in the same manner. As the dynamic recording range of the seismograph is limited, the magnitude of the events analyzed increases with the distance on the average, apparently resulting in an increase in the amount of attenuation. In order to reduce this effect we also calculated the slope for the range of magnitude from 2.8 to 3.6. In Table 3 the values of Q^{-1} for the various cases above are listed. These were calculated under the assumption of the independence of Q from the frequency, that is,

$$Q = -\frac{\pi(f_1 - f_2)}{v\{\gamma(f_1) - \gamma(f_2)\}} \tag{7}$$

, where we use $v_p = 6.5$ km/sec and $v_s = 3.6$ km/sec.

The values of Q^{-1} for the narrow range of magnitude are lower than those obtained with all data, reducing the effect of the variation of the source spectra with the magnitude. However, there is a 20~30% difference in the two cases, one of

Table 3. Q^{-1} Estimated with the Amplitude Ratio of the Different Frequency Bands.

	f_1Hz/f_2Hz	$2.3 \leq M \leq 4.9$		$2.8 \leq M \leq 3.6$					
		$R \leq 200$ Km		$R \leq 200$ Km			$R \leq 175$ Km		
		N	$Q^{-1}(\times 10^{-2})$	N	$Q^{-1}(\times 10^{-2})$	q	N	$Q^{-1}(\times 10^{-2})$	q
P	8/1.2	56	0.368 ± 0.012	37	0.340 ± 0.003	75	35	0.383 ± 0.013	66
	16/4	146	0.135 ± 0.005	102	0.103 ± 0.007	189	76	0.111 ± 0.014	175
S	8/1.2	87	0.274 ± 0.004	64	0.241 ± 0.006	106	61	0.225 ± 0.008	113
	16/4	141	0.144 ± 0.001	105	0.135 ± 0.001	143	84	0.181 ± 0.001	107

which excludes the earthquake swarm near the Ontake-volcano, while the other contains all datas. Therefore the results obtained in this method must have an error amounting to 20~30%, although the standard deviations calculated are fairly small.

In both cases of P and S, the values of Q^{-1} for 8 Hz/1.2 Hz are larger than those for 14 Hz/2 Hz. The difference between them exceeds the above range of error, suggesting the tendency of an increase of Q with frequency. This tendency is same as the dependence of Q_s on the frequency obtained in the section 3–1.

Assuming $Q=q\sqrt{f}$ for the body wave instead of the constant Q like the attenuation of the coda, we obtain

$$q = \frac{\pi(\sqrt{f_1}-\sqrt{f_2})}{v\{\gamma(f_1)-\gamma(f_2)\}}. \tag{8}$$

The values of q are listed in Table 3. For P wave the value of q changes rather largely according to the frequency bands used. For S wave nearly same values are obtained, with the mean of $q=110$. As the same tendency concerning the dependency of Q_s on the frequency can be derived with quite different ways (Tables 2 and 3), it is considered reasonable to use the relation of $Q_s=110\sqrt{f}$ for the attenuation of the S wave in the crust in and around the Kinki district.

4. Source spectral density and regional variation.

In order to derive the absolute value of the spectral density for the far-field

Table 4. List of the Events used for the Reference Earthquake.

No.	Y Code	Date	Time	Hypocentral Azimuth N°E	Hypocentral Distance Km	Magnitude
1	78- 797	Aug. 23	12:41	−25°	24.2	2.2
2	78-1106	Oct. 13	7:31	−128	10.9	2.1
3	79- 571	Apr. 19	19:57	−82	15.0	2.2
4	79- 639	May 4	11:06	70	9.2	1.7
5	79-1033	Aug. 18	20:20	−167	15.7	2.3

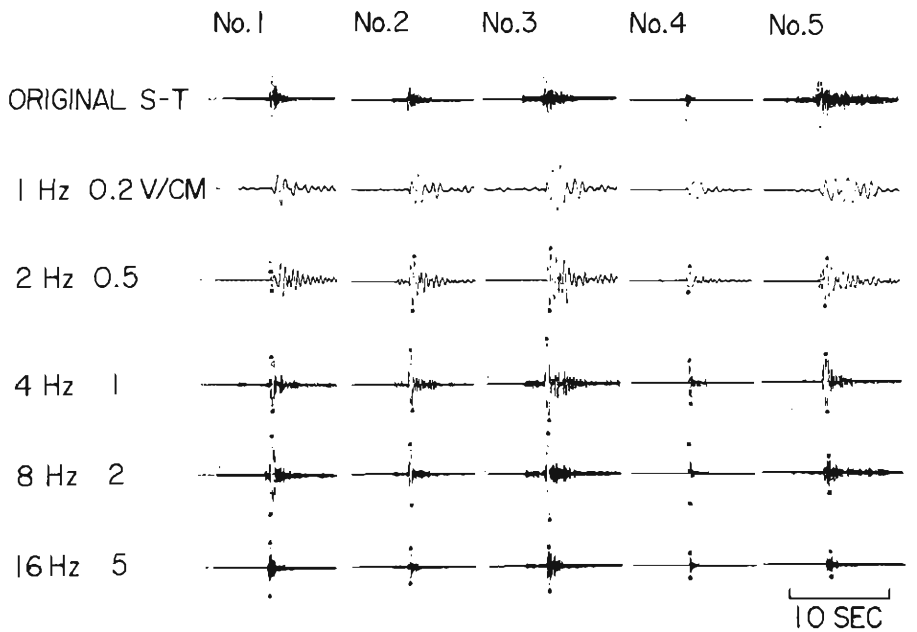

Fig. 11. The wavelets of the band pass filtered seismograms which are used for the reference earthquake. The maximum amplitude in the transversal component of the S waves (dotted) are used to make the spectral densities in Fig. 12.

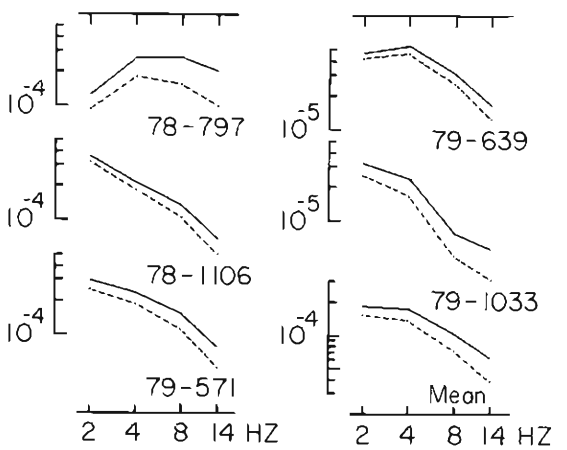

Fig. 12. The displacement spectral density of SH normalized to the hypocentral distance of 1 km, reduced by 2 for surface reflection. Q_s is given by $110\sqrt{f}$. The broken line represents the ones whose spectra are uncorrected for Q_s.

shear wave from the source factor of coda, the calibration of the coda level is necessary for at least one event. As the relation of the coda source factor to the magnitude is linear in the range of magnitude, $M=2\sim5$ (Fig. 5), the source spectral densities are obtainable for all events by a reference earthquake with some fixed magnitude. The reference earthquake was obtained in the following way.

As a rough approximation the amplitude of a wavelet through a band pass filter is the product of its amplitude spectral density and twice the band width[3]. With this relation we obtained the shear spectral densities of the nearest events from their transversal components. The events used are listed in Table 4, and the forms of the wavelets and their spectral densities are shown in Figs. 11 and 12. The attenuation of the S wave is given by $Q_s=110\sqrt{f}$, and the spectral densities are normalized to the hypocentral distance of 1 km. The spectra uncorrected for Q_s are also shown in Fig. 12. The spectral shapes do not change extremely by attenuation, because of the short hypocentral distance and the relatively high Q at the high frequency range. The variation of the spectral shapes from event to event is much larger than those from the effect of Q_s. Allowing this variation as a deviation, the mean spectral density was obtained, as shown in Fig. 12, and was used for the reference earthquake with $M=2.1$.

Assuming the ω-square model for the spectral density of the far-field shear wave[9], the ω-square curve was fitted to the above reference spectra, and the absolute value of the spectral density for each pass band was estimated by the curve, as shown at the bottom of Fig. 13. The scales for the spectral density in cm·sec at the left side of Fig. 5. were decided with the above mentioned procedure and were used for the transformation of the coda source factor to the source spectral density of the far-field shear wave normalized at the distance of 1 km.

Fig. 13 shows the source spectral densities when M is 3, 4 and 5 (○). It is remarkable that all spectra are explained fairly well by the ω-square curve.

As shown in Fig. 4 the source factor

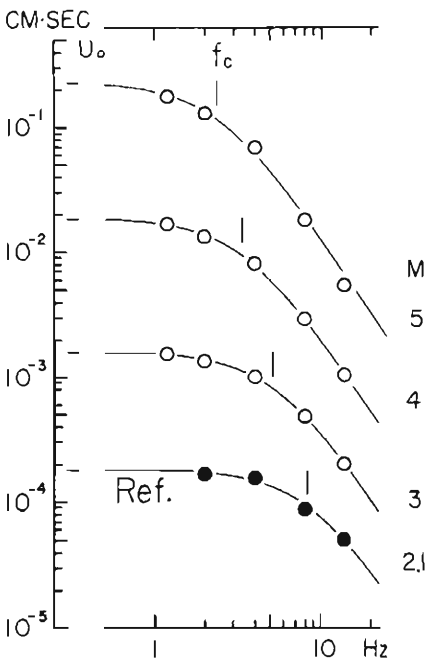

Fig. 13. Source spectral densities of $M=3$, 4 and 5 derived from the general growth of the source factor of coda in Fig. 5. The bottom one (●) is the reference spectra in Fig. 12. Note that the ω-square curves are fitted fairty wetl to all the spectra in the range of $M=2\sim5$.

of coda varies with the source location systematically, suggesting regional variation of the source spectra. We proposed to estimate the source parameters for each event by fitting the ω-square curve to each source spectral density obtained from the source factor of coda.

Fig. 14 shows the source spectral densities of the shear waves at 1 km, which are grouped by the source region and depth corresponding to Table 1. The error bars of the spectral densities are those of the coda source factors. They were estimated when eq. (4) was fitted to the coda amplitude $A(f, t)$ by the least square method. The amount of the error depends on the fluctuation of the coda amplitude and the length of the time interval used for the analysis. The ω-square curves in Fig. 14 were fitted manually by a graphic method, from which the shear displacement level at the zero frequency, U_0, and the corner frequency, f_c, were determined for each event.

The seismic moment, M_0, is related to the shear displacement spectral level, U_0,

$$M_0 = 4\pi\rho v_s^3 U_0 R/R_{\theta\varphi} \tag{9}$$

, where ρ: density, v_s: shear wave velocity, R: hypocentral distance and $R_{\theta\varphi}$: radiation pattern[10]. The values of M_0 were estimated with $\rho=2.9$ gr/cm^3, $v_s=3.6$ km/sec, $R=1$ km and $R_{\theta\varphi}=1/\sqrt{2}$ for the geometrical mean, and are listed in Table 1 together with f_c. According to Brune's model of dislocation, the radius of the equivalent circular dislocation surface, r, is related to the corner frequency, f_c, of the displacement spectral density of the far-field shear wave[11,12],

$$r = 2.34\, v_s / 2\pi f_c \tag{10}$$

The stress drop, $\Delta\sigma$, is given by

$$\Delta\sigma = 7\, M_0/16\, r^3 \tag{11}$$

The values of r and $\Delta\sigma$ estimated are also listed in Table 1.

The relation between f_c and M_0 is shown in Fig. 15 with the symbols for the source regions, in which the scale for the source dimension, $2r$, and the constant stress drop lines have been added[13]. In the figure the slope of the lines is 3 by definition. Some tendencies of the source characteristics and the scaling law can be obtained from the figure. That is, in the range of magnitude smaller than about 3, the slope of the relation between M_0 and f_c is much steeper than 3. As a result the amount of stress drop increases from a few bars to about 10 bars with increase of moment. In the range of $M=3\sim5$, however, the slope is nearly 3. The amount of $\Delta\sigma$ varies with events ranging from 10 to 100 bars. This non-linear relation between M_0 and f_c in the log-log scale is similar to those of an other investigation[5].

In addition to the above general tendency for this area, it is very remarkable that the relation between M_0 and f_c varies systematically with the source location. That is, the corner frequencies of the shallow events in a swarm near Wakayama

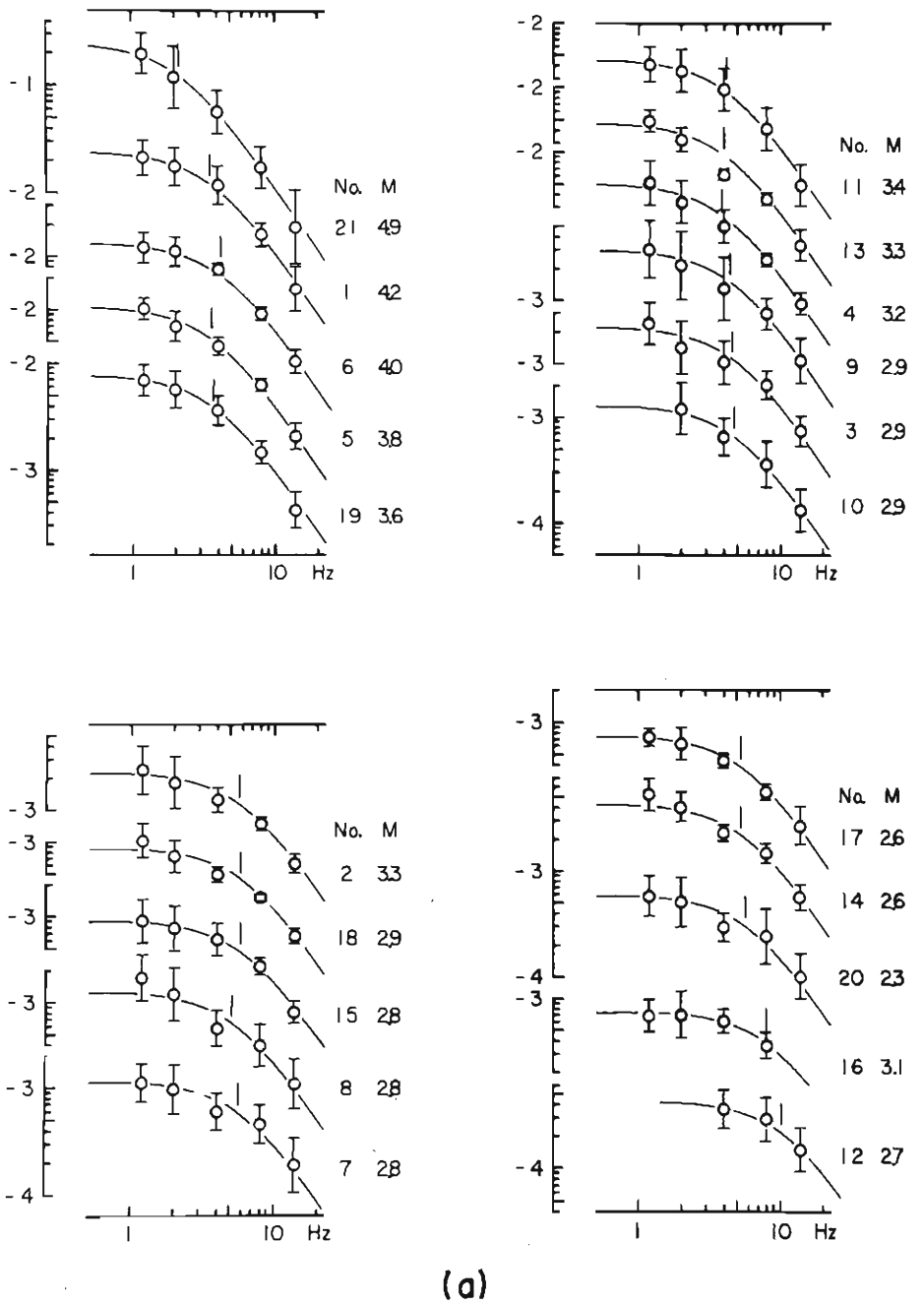

Fig. 14. Source spectral density of each event derived from the source factor of coda. (a) Region of the Yodogawa seismic zone.

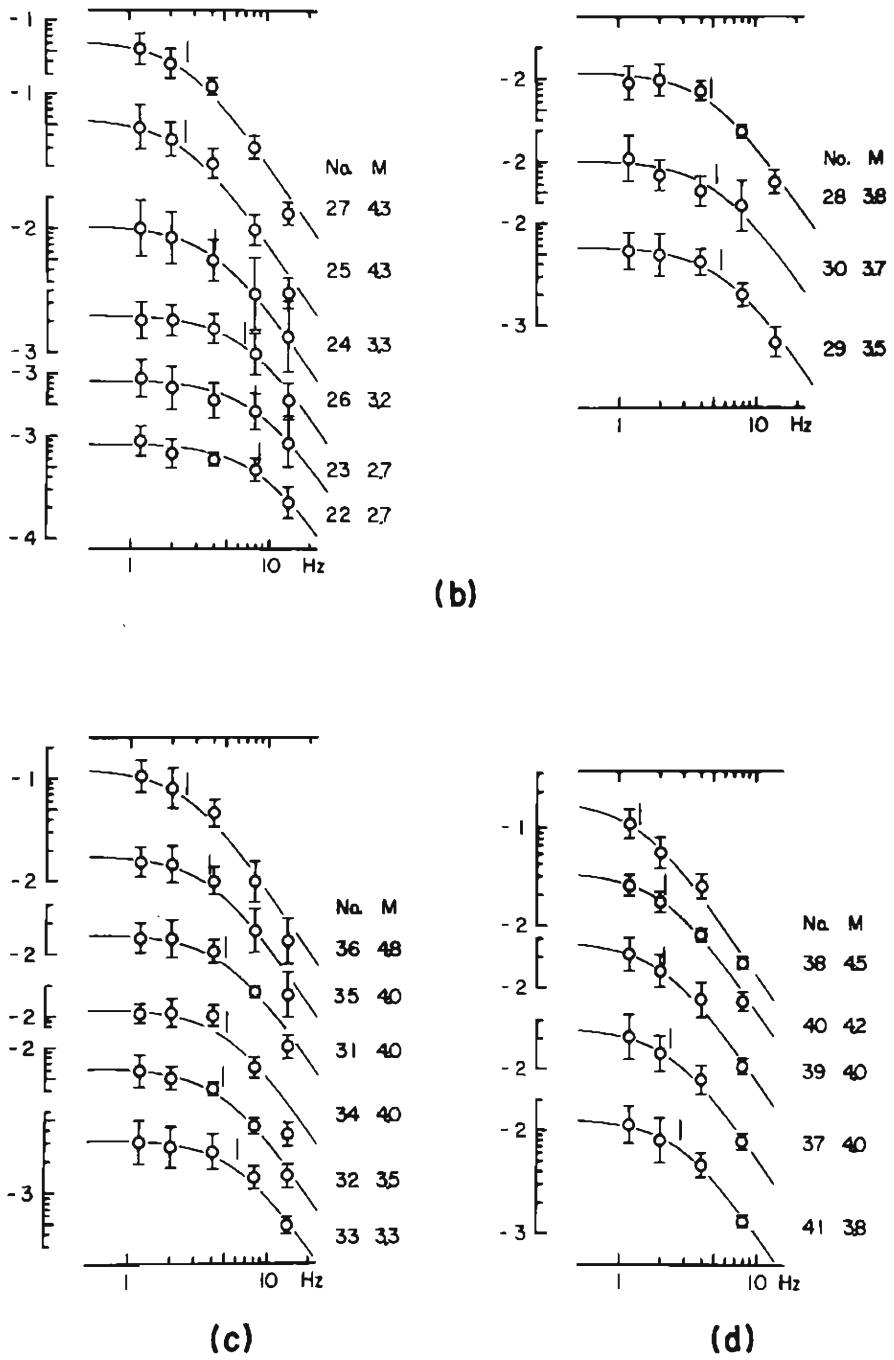

Fig. 14. continued. (b) Region of Iga-ueno, Nara and NW Mie prefectures, (c) region of Yoshino, Nara-Wakayama border, (d) near Wakayama city.

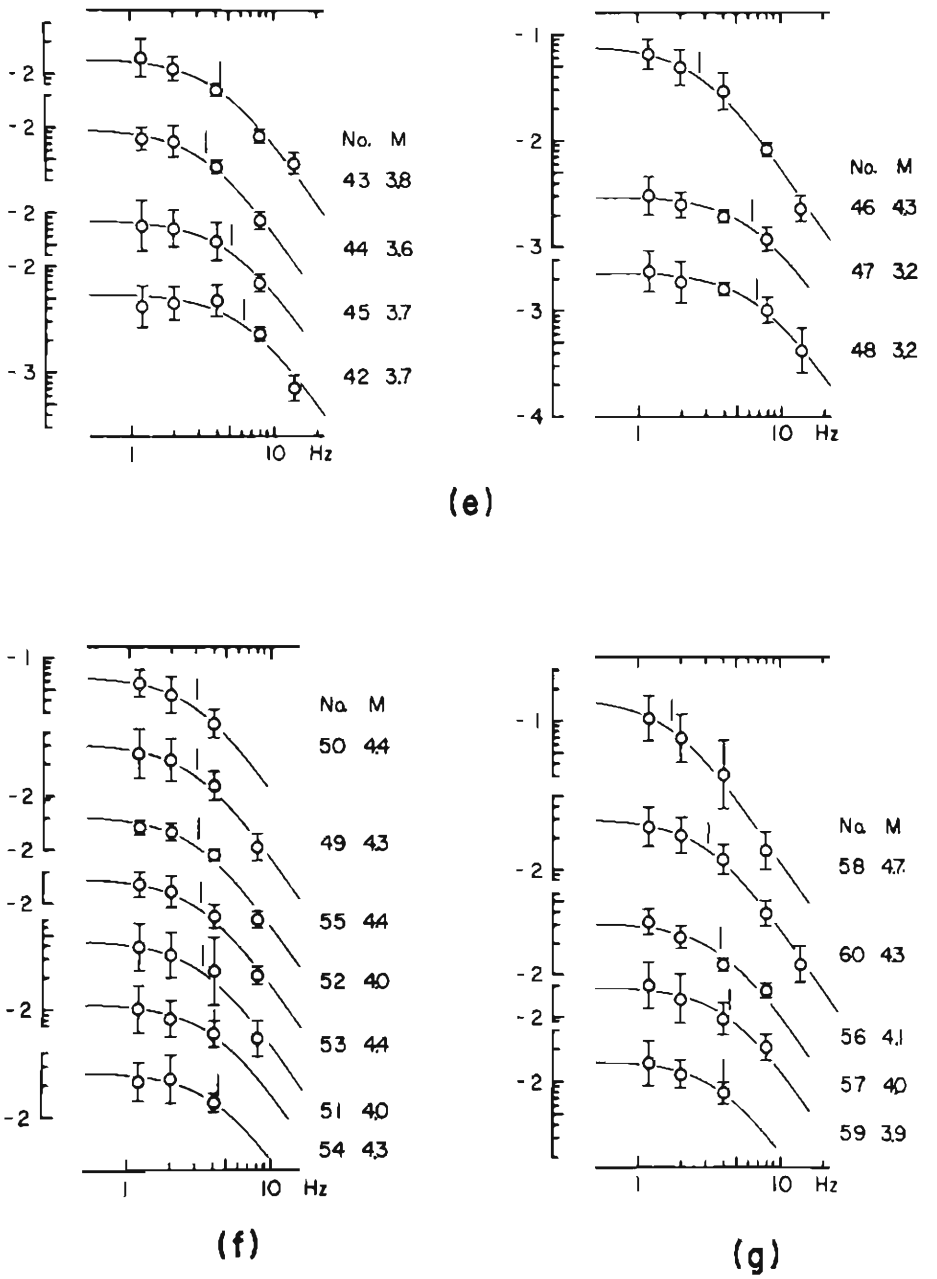

Fig. 14. continued. (e) Gifu and Aichi prefectures, (f) in and off Kii peninsula and Kii channel, (g) others including the events near the Ontake-volcano.

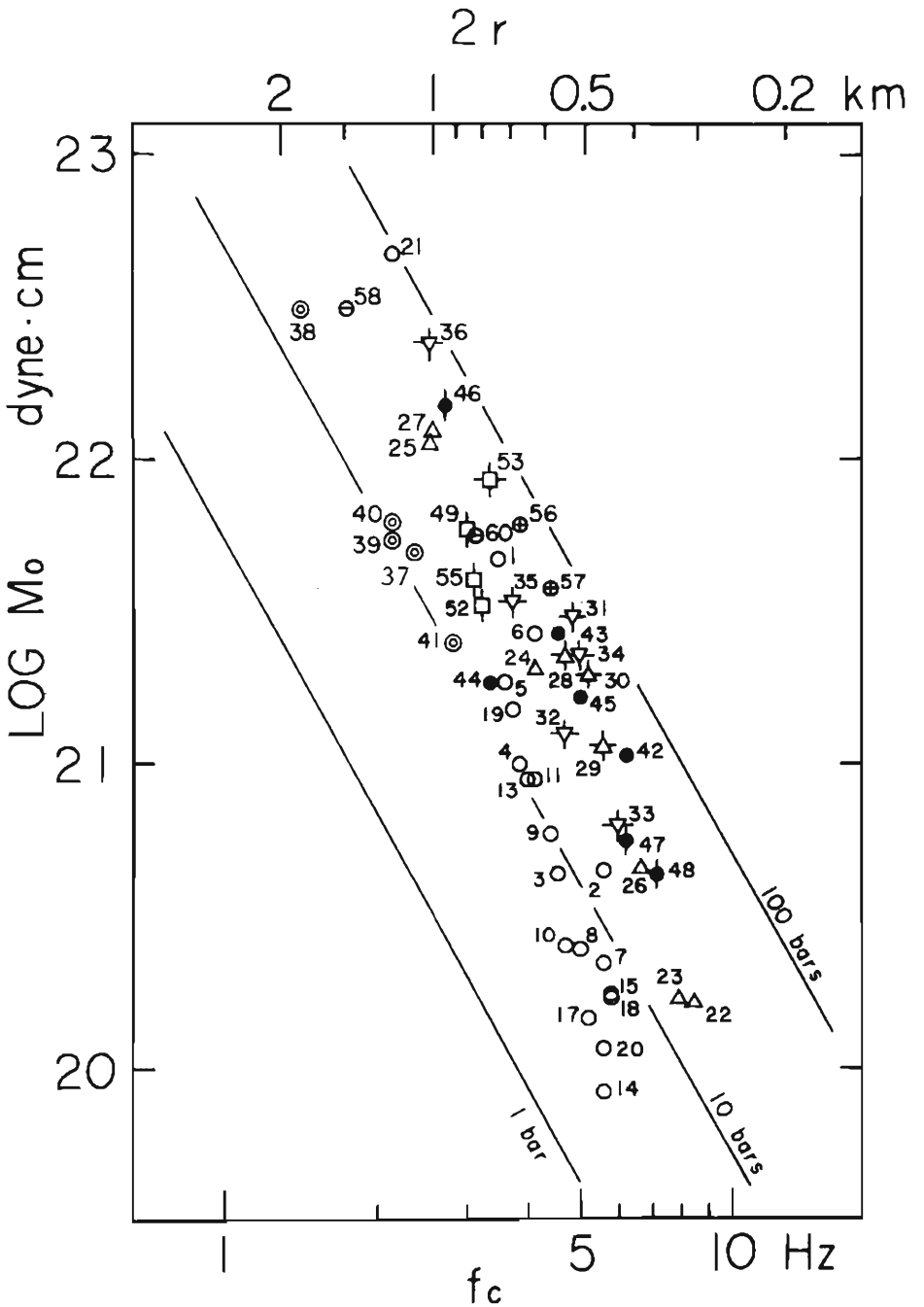

Fig. 15. Relation between the seismic moment and the corner frequency. Note that the relation changes at about $M=3$ (log $M_0 \simeq 21$). The scale in Km units is for the diameter of the equivalent circular dislocation. The lines of the constant stress drop are also estimated from Brune's model.

city (◎) and those in the Yodogawa seismic zone (○) are lower than the frequencies of the events with same level of M_0 in other regions. Therefore the events in the two regions are characterized by a relatively low stress drop. On the contrary, events in the region of Nara and Mie prefectures (△), which is known as a relatively non-active region in seismicity, show high values of stress drop. The deeper events in this region (△) and the Yoshino region (▽) also show high values. The deeper events in and off the Kii peninsula and in the Kii channel (□) are also characterized by a relatively high stress drop.

As the value of the stress drop depends on the cube of the values of f_c, some amount of uncertainty in the absolute value of $\Delta\sigma$ is unavoidable. However, the regional variation of the source characteristics is the same as those discussed with the source factor of coda whose error limit could be reasonably estimated (Fig. 4).

5. Discussion.

As is discussed in detail in a previous paper[6], Q of the seismic coda depends both on the frequency and on the lapse time. Assuming $Q=q\sqrt{f}$, we may estimate q for the various intervals of the lapse time as listed in Table 5 (see Table 3 of the paper[6]). The value of q for the coda increases gradually with the lapse time from 130 to 220.

Q_s for the S wave is also approximated with $Q=110\sqrt{f}$ within the range of distance from 20 to 175 km, which corresponds to the range of the S arrival time from 5 to 50 sec, as discussed in section 3.

Okano and Hirano discussed the attenuation property of the body waves in the crust in the vicinity of Kyoto[14]. From the attenuation of the amplitude ratios of the two recording systems with different frequency responses, they obtained $Q_s=850$ under an assumption of the constant Q for the most probable value. They also suggested that Q may increase with frequency from the analysis of the variation in the predominant frequency with distance. The result, $Q_s=850$, may be equivalent to $q=116$ under the assumption of $Q=q\sqrt{f}$, with $f_1=2.5$ Hz and $f_2=33$ Hz of their systems for the distance of 40～160 km, or about $t_s=10$～45 sec.

From these observations, we are convinced that Q of the body wave in the frequency range of 1～30 Hz in the crust increases with frequency quite similarly to that of the seismic coda. Most recently Rautian et al. discussed Q_s and its dependency on the frequency with the CHISS seismograms[15]. Their result is, in a wide range of frequency from 0.2 to 40 Hz, $Q_s=360\sqrt{f}$ for $t_s=8$～200 sec, and $Q_s=70\sqrt{f}$ for $t_s=2$～8 sec in Garm region, which resembles the above result.

Table 5. q for the Coda Parts.

T sec	15－45	20－60	40－90	60－120	80－150
q	131±9	159±14	216±16	217±15	212±24

As the attenuation property of the S wave is quite similar to that of the coda parts, it is suporsed that the same physical mechanism of the attenuation is applicable to them; that is, the loss of energy by wave scattering and the intrinsic absorption of the medium. In the frequency range of 1∼20 Hz, wave scattering may be reasonably considered to be caused by the heterogeneity existing in the upper lithosphere[16,17]. In the previous paper[6] the fluctuation of the coda amplitude was examined to estimate the loss of energy by scattering, from which the dependence of the apparent attenuation on frequency cannot be explained. Consequently, we have no reasonable physical models giving a frequency dependent Q like $Q=q\sqrt{f}$. In the practical sense, however, it is suggested that the regional attenuation property of the S wave for the upper lithoshere may be examined rather easily with high resolution by the analysis of the seismic coda in the frequency range which is important to pure and applied seismology.

The source characteristics of small earthquakes occuring near Kyoto were discussed from the spectral densities of the body waves. Furuzawa et al. showed that the predominant frequencies in the spectra of the body waves for the microearthquakes in the Yodogawa seismic zone are lower than those for Nara region, where the seismic activity is relatively low[1]. Their observational result corresponds to the result that the events in the seismically active region are characterized with low stress drop in the amount of 0.2∼0.5 times than those of the non-active region (Table 1 and Fig. 15).

Hirano discussed the regional variation of the stress concentration with the spectral analysis of low magnification seismograms, suggesting that in the Yodogawa seismis zone the northern parts, where the aftershock activity and the seismicity are relatively low, are characterized by high stress concentration than the southern parts[2]. In the analysis of the coda, the event with the highest stress drop (No. 21) is located at the northern end of the zone.

The source characteristics of the shallow earthquakes near Wakayama city were studied with the seismic coda[5] and the spectral analysis of the body waves[18]. In the coda analysis the event in the region near Wakayama city (◎) are very conspicuous by the low stress drop. Nearly the same results were obtained as those from the coda by Chouet et al.[5]. As for the corner frequency, which is considered to contain some large amount of uncertainty, the results obtained in the range of the epicentral distance of 80–110 km are lower only by the amount of 0.14 in the logarithmic frequency than the results obtained in their source region[5]. Therefore, the analysis of the seismic coda to examine the source characteristics is considered possible not only in the source region, but also in the wider circumferential area, as long as the lapse time is sufficiently long.

The events, Nos. 56 and 57, located at SW Nagano prefecture (⊕), show a different nature; that is, the high stress drop in spite of the high seismic activity in a swarm. In the analysis of the amplitude ratio of the body waves, the high frequency components are very large compared with those of other regions as shown

in Fig. 10. This earthwauke swarm, occurring from August 1976, has attracted geophysical interest in connection with the abruct eruption of the Ontake-volcano on Oct. 28, 1979[19]. Allowing this region to be an exception it is supposed that a seismically active region where small and micro earthquakes ($M<5$) occur frequently can be characterized by a low stress drop, or perhaps by the low strength of the rock in the upper crust.

As regional variation is conspicuous, the variation of the stress drop with the source depth is not clear. However, the deeper events of $H \geqq 40$ km show relatively high values of $\Delta\sigma > 25$ bars. On the other hand for the shallower events ($H \leqq 20$ km) $\Delta\sigma$ falls in the range of $10 \sim 100$ bars.

The discussion of the source characteristics has been based mainly on two arguments, one of which is the observational result that the source factor of coda increases linearly with magnitude in the range of $M=2 \sim 5$ (Fig. 5), and the other is the assumption that the ω-square model is applicable to the source spectral density of the far-field shear wave. As the first step in the analysis, the ω-square curve was fitted to the reference spectra of $M=2.1$, but this was done using only 4 points (Fig. 13). Therefore, in this stage the other model such as the ω model might be applicable[20]. If we use the ω model for the reference earthquake, however, the spectral density of $M=5$ decreases with $\omega^{-1.5} \sim \omega^{-2}$ in the higher frequency range above 2 Hz, which cannot be explained by the same ω model. As shown in Fig. 13 the average spectral densities are approximated fairly well by the ω-square model up to $M=5$.

When seismic scaling is discussed, the observational result, wherein the spectral level decreases with ω^{-2} in the higher frequency range, is very important in connection with the attenuation property discussed above (i.e. $Q=q\sqrt{f}$). Because of the large value of Q, that is, the small attenuation in the higher frequency range, the source spectral density estimated by the observed body wave shows a lower level in the higher frequency range than those estimated by constant Q. Therefore the ω-square model, which was proposed originally to explain the sourec spectra for larger event of $M>6$, may be applicable in the lower range of $M=2 \sim 5$[5,21].

On the other hand, in engineering seismology the maximum acceleration of a synthetic seismogram will be underestimated in the higher frequency range when the value of Q is given as constant. Nuttli showed that the apparent Q is 1500 for the 10 Hz Lg wave, and took notice of the damage potential of the wave[22]. In the estimation of the seismic risk from a synthetic seismogram, it is necessary to consider the dependency of the attenuation on frequency like $Q=q\sqrt{f}$.

6. Conclusion.

The attenuation property of the seismic waves and the source characteristics of small earthquakes were discussed analyzing the body waves and the coda parts.

The values of Q for P and S waves vary with the frequency systematically in the range of $1 \sim 20$ Hz. Q_s is approximated by $Q_s=110\sqrt{f}$ for the S travel time of

$t_s=5\sim50$ sec, which is identical with the attenuation property of the seismic coda. The attenuation of the body waves from the local earthquakes is inferred to be affected by the scattering process to the same degree as the coda. It is suggested that the regional attenuation property and its variation with the depth can be estimated by the analysis of the coda parts of the seismograms.

The estimated source spectral density of the far-field shear wave is approximated fairly well by the ω-square model in the magnitude range of $M=2\sim5$. However, the general tendency of the relation between the seismic moment and the corner frequency changes at about $M=3$. In the range of $M<3$, the amount of stress drop, estimated with Brune's model of dislocation, increases with magnitude from a few bars to several tens of bars. In the range of $3<M<5$, the stress drop is $10\sim$ 100 bars, varying with the source location. In the Kinki district, shallow events occurring in the seismically active regions such as those near Wakayama city and the Yodogawa seismic zone are characterized by low stress drop compared with the other non-active regions.

The examination of the seismic coda is available to study the source characteristics not only in the source region but also in a wider area, as long as the lapse time is sufficiently long.

In the discussion of the source characteristics and seismic scaling from observation, and in the estimation of the seismic risk from a synthetic seismogram, it is necessary to consider the dependency of the attenuation on frequency like $Q=q\sqrt{f}$.

Acknowledgement

The author wishes to express his sincere thanks to Prof. Soji Yoshikawa of Kyoto University for his encouragement, and also to Dr. Tamotsu Furuzawa for his most valuable advice in carrying out this work. The author is indebted to Messrs. Masao Nishi and Toshio Kobayashi for their helpful assistance with observation and Miss Kazue Segawa for her help.

The data processing was run on a FACOM M-130 at the Information Data Processing Center for Disaster Prevention Research, of the Disaster Prevention Research Institute of Kyoto University.

Comment added in the proofreading

In a previous paper[6], the property of fluctuation in the logarithmic amplitude of coda was discussed in connection with turbidity. In this respect, Aki pointed out in his letter that the fluctuation of seismic coda cannot be connected with turbidity, because it has been saturated already. Following the theory of sound transmission through a fluctuating ocean[23], a boundary between the unsaturated and saturated regions of the amplitude fluctuation can be estimated to be about 45 sec for 1 Hz S wave, when we assume the 1% deviation of S velocity ($v_s=$

3.5 km/sec) and the correlation length of 30 km. Therefore, the coda parts used in the analysis ($t=15\sim300$ sec) may be in the transitional zone from the unsaturated region to saturated one of the amplitude fluctuation. The amount of the scattering loss of energy was also estimated with the turbidity coefficient. The proportion of scattering loss in the total attenuation was obtained to be about $1\sim6\%$. As the coda was considered to be generated by wave scattering, scattering loss was suspected to play a important role in the attenuation. This discrepancy may be attributable to the underestimation of turbidity coefficient because of the saturation of fluctuation in the seismic coda.

The author wishes to express his sincere thanks to Prof. Keiichi Aki of Massachusetts Institute of Technology for his kind indication. (Nov. 25, 1980)

Reference

1) Furuzawa, T., K. Irikura and J. Akamatsu: Regional Variation of Body Waves' Spectra from Small Earthquakes Occurring in the Southern Parts of Kyoto, Zisin, Vol. 26, 1973, pp. 275–284 (in Japanese).
2) Hirano, I.: Source Characteristics of the Earthquakes Occurring in the Vicinity of Kyoto, Bull. Disas. Prev. Res. Inst., Kyoto Univ., Vol. 24, 1974, pp. 67–80.
3) Aki, K. and B. Chouet: Origin of Coda Wave: Source, Attenuation, and Scattering Effects, J. Geophys. Res., Vol. 80, 1975, pp. 3322–3342.
4) Rautian, t. and V. I. Khalturin: The Use of Coda for Determination of the Earthquake Source Spectrum, Bull. Seism. Soc. Am., Vol. 68, 1978, pp. 923–948.
5) Chouet, B., K. Aki and M. Tsujiura: Regional Variation of the Scaling Law for Earthquake Source Spectra, Bull. Seism. Soc. Am., Vol. 68, 1978, pp. 49–79.
6) Akamatsu, J.: Attenuation Property of Coda Parts of Seismic Waves from Local Earthquakes, Bull. Disas. Prev. Res. Inst., Kyoto Univ., Vol. 30, 1980, pp. 1–16.
7) Akamatsu, J.: Seismic Observation at the Sumiyama Seismic Station (2), Annuals of Disas. Prev. Res. Inst., Kyoto Univ., No. 23B-1, 1980, pp. 107–114 (in Japanese).
8) Akamatsu, J.: Seismic observation at the Sumiayma Seismic Station (1), Annuals of Disas. Prev. Res. Inst., Kyoto Univ., No. 20B-1, 1977, pp. 13–19 (in Japanese).
9) Aki, K.: Scaling Law of Seismic Spectrum, J. Geophys. Res., Vol. 72, 1967, pp. 1217–1231.
10) Keilis-Borok, V. I.: Investigation of the Mechanism of Earthquakes, Trudy Inst. Geofis. Akad. Nauk., SSSR, No. 40, 1957 (in Russian), English Transl., Soviet Res. Geophys. Ser., Vol. 4, 1960.
11) Brune, J. N.: Tectonic Stress and the Spectra of Seismic Shear Waves from Earthquakes, J. Geophys. Res., Vol. 75, 1970, pp. 4997–5009.
12) Brune, J. N.: Correction, J. Geophys. Res., Vol. 76, 1971, p. 5002.
13) Hanks, C. N. and W. Thatcher: A Graphical Representation of Seismic Source Parameters, J. Geophys. Res., Vol. 77, 1972, pp. 4393–4405.
14) Okano, K. and I. Hirano: Seismic Wave Attenuation in the Vicinity of Kyoto, Bull. Disas. Prev. Res. Inst., Kyoto Univ., Vol. 21, 1971, pp. 99–108.
15) Rautian, T., V. I. Khalturin and M. S. Zakirov: Study of Conditions in Source Regions with Seismic Coda, Physical Process in Earthquake Sources, Nauka Publishing Hause, Moscow, 1980, pp. 224–256 (in Russian).
16) Aki, K.: Scattering of P Waves under the Montana Lasa, J. Geophys. Res., Vol. 78, 1973, pp. 1334–1346.
17) Aki, K.: Analysis of the Seismic Coda of Local Earthquakes as Scattered Waves, J. Geophys. Res., Vol. 74, 1969, pp. 615–631.

18) Ishida, M.: Determination of Fault Parameters of Small Earthquakes in the Kii Peninsula, J. Phys. Earth, Vol. 22, 1974, pp. 177–212.
19) Aoki, H., T. Ooida and F. Yamazaki: Earthquake swarm in the Southern Foot of Mt. Ontake, Bull. Volcano. Soc. Japan, Vol. 25, 1980, p. 106 (Abstract for the Meeting, in Japanese).
20) Brune, J. N. and C. Y. King: Excitation of Mantle Rayleigh Waves of Period 100 seconds as a Function of Magnitude, Bull. Seism. Soc. Am., Vol. 57, 1967, pp. 1355–1365.
21) Aki, K.: Scaling Law of the Earthquake Source Time-Function, Geophys. J. R. astr. Soc., Vol. 31, 1972, pp. 3–25.
22) Nuttli, O. W.: A Time-Domain Study of the Attenuation of 10-Hz Waves in the New Madrid Seismic Zone, Bull. Seism. Soc. Am., Vol. 68, 1978, pp. 343–355.
23) Flatte, S. M., R. Dashen, W. H. Munk, K. M. Watson and F. Zachariasen: Sound Transmission through a Fluctuating Ocean, Cambridge University Press, 1979, pp. 85–161.